Antimicrobial and corrosion inhibition studies of homoleptic metal (II) complexes of fluoroaniline schiff base: Synthesis, and characterization

Scientific Modelling and Research
Vol. 9, No. 1, 69-88, 2024
e-ISSN: 2523-952X

(✉ *Corresponding Author)*

Amadi, Jane Uchechi[1]
Festus, Chioma[2]

[1,2]*Department of Chemistry, Faculty of Natural and Applied Sciences, Ignatius Ajuru University of Education, Rivers State, Nigeria.*
[1]*Email: amadijane99@gmail.com*
[2]*Email: chioma.festus@iaue.edu.ng*

ABSTRACT

A Schiff base ligand, HL derived from 4-fluoroaniline and 2-hydroxy-1-nalphaldehyde was reacted with acetate salts of Cu(II), Zn(II), Co(II), Mn(II), Ni(II) and Fe(II) sulfate to give their corresponding metal(II) complexes. The synthesized compounds were characterized via analytical methods, spectral assessments; and were applied as corrosion inhibitors. The Fourier Transformation Infrared (FTIR) spectrum of HL presented a band at 1632cm^{-1} which were observed within 1623-1630 cm^{-1} in the spectra of the complexes; and was apportioned to an azomethine moiety. The electronic (UV-vis) studies showed that complexes displayed octahedral geometries with various transitions within the synthesized compounds. The ligand and its metal complexes were completely soluble in C_2H_6OS, and C_3H_7NO but was sparingly soluble in CH_3Cl except for Fe(II) and Co(II) which were insoluble and completely soluble respectively. Divalent iron, nickel, copper and zinc complexes exhibited high melting points (240-285°C) and different shades of brown, except for nickel which was olive green. The ligand melted at 160°C. The Cu(II) complex show high activity against *Bicilus cerus* (11.0 ± 1.41) and mild activity against *S. aueus, P. aeruginosa, K. pneumonia* (6.5 ± 0.71, 4.0 ± 0.0, 2.0 ± 2.82) respectively and no activity against *proteus mirabilis.* The compounds were found to be inactive against *K. Pneumonia* except for iron(II) and copper(II) complexes. However, outstanding antifungal actions were acquired for the compounds against *Aspergillus flavus, fuserium sp. and Aspergillus Niger.* The ligand with its bivalent complexes also presented substantial corrosion inhibition behaviour in opposition to corrosion of mild steel in aggressive HCl solution with values ranging from 68% to 91% at different hours.

Keywords: *2-hydroxy-1-nalphaldehyde, Antimicrobial inhibition, Characterization, Schiff bases, HL(ligand).*

DOI: 10.55284/smr.v9i1.1276
Citation | Uchechi, A. J., & Chioma, F. (2024). Antimicrobial and corrosion inhibition studies of homoleptic metal (II) complexes of fluoroaniline schiff base: Synthesis, and characterization. *Scientific Modelling and Research, 9*(1), 69–88.

Funding: This study received no specific financial support.
Institutional Review Board Statement: Not applicable.
Transparency: The authors confirm that the manuscript is an honest, accurate, and transparent account of the study; that no vital features of the study have been omitted; and that any discrepancies from the study as planned have been explained. This study followed all ethical practices during writing.
Competing Interests: The authors declare that they have no competing interests.
Authors' Contributions: Both authors contributed equally to the conception and design of the study. Both authors have read and agreed to the published version of the manuscript.
History: Received: 28 October 2024/ Revised: 3 December 2024/ Accepted: 16 December 2024/ Published: 27 December 2024
Publisher: Online Science Publishing

Highlights of this paper

- The amine compound 4-fluoroaniline was reacted with 2-hydroxyl-1-naphthaladehyde to give the Schiff base ligand which was reacted with some selected metal salts.
- The synthesized metal complexes were characterized using various analytical and spectroscopic techniques (e.g., UV-Vis spectroscopy, FTIR, NMR) to confirm their molecular structure and the formation of metal complexes.
- The anti-microbial activity of the synthesized metal complexes were evaluated against a range of microorganisms and the corrosion inhibition properties of the metal complexes were assessed.

1. INTRODUCTION

Metal complexes and organic molecules have received increasing attention as they have been used as pharmacophores in the medical and pharmaceutical fields [1]. Basically, the presence of multiple functional groups in molecules improves their properties when directed in essential fields such as medical and industrial [2]. Schiff base (azomethine) group of compounds are one of the compounds that have had major significance over the past decades until now [3]. An assortment of ligand type of Schiff-bases and their metal complexes have been separated, these compounds have very malleable and various structures. Therefore, their properties have been studied [4].

A German chemist, Hugo Schiff first synthesized Schiff base in 1864 which are compounds containing -C=N- group. They are usually prepared by the condensation of primary amines and active carbonyl groups [5]. They are topflight coordinating ligands that forms stable complexes with various transition metal ions [6]. Nowadays, Schiff bases are used as intermediates for the synthesis of amino acids or as ligands for the preparation of metal complexes having a series of different structures [7]. Schiff bases with acyl substituents are more stable and readily synthesized, whereas those containing alkyl substituent are relatively unstable [7]. Schiff bases of aliphatic aldehydes are unstable and readily polymerizable while those with aromatic aldehydes having effective conjugation are more stable [8]. Schiff base as an interesting class of ligands have played significant role in the betterment of coordination chemistry. Schiff bases and their complexes have a diversity of applications in biological activity studies and industry [9]. Till date, they are used as radiotracers in nuclear medicine and drugs [10]. Moreover, Schiff bases are extremely momentous substances for inorganic chemists as these are generally used in medicinal inorganic chemistry because of their various biological, pharmacological, antitumor activities as well as their outstanding chelating ability [11]. Furthermore, they have applications in many fields such as biological (including antibacterial, antifungal, anti-oxidative, anti-inflammatory, anti-tumor, anti-cancer and anti-HIV), optical materials, chemical sensor, clinical, analytical, and electrochemistry [12]. Mixed ligand complexes have a major role in the biological field as shown by several ways in which metal ions activate enzymes. Schiff bases derived from heterocyclic compounds, P-anisaldehyde and furan-2-carbaldehyde have attracted keen interest in biological chemistry [13].

2. EXPERIMENTAL DETAILS

2.1. Materials

2-hydroxyl-1-naphthaldehyde, 4-fluoroaniline manganese (II) acetate tetrahydrate, iron (II) tetraoxosulphate heptahydrate, cobalt (II) chloridehexahydrate, nickel (II) acetatetetrahydrate, copper (II) acetatedihydrate, zinc (II) acetatedihydrate, distilled water, acetic acid, triethylamine, ethanol, chloroform, methanol, dichloromethane, acetone, hydrochloric acid, drying agent, N,N'-dimethylformamide (C_3H_7NO), and dimethylsulfoxide (C_2H_6OS) were used as received from the supplier (Bristol scientific).

2.2. Characterization

The melting/decomposition points of the azomethine based chelator and its metal(II)complexes were obtained using a transparent cut-glass capillary hosepipe in the electrochemical melting point machine. The infrared spectra of the compounds were recorded using a PerkinElmer Infrared Spectrophotometer between 4000–400 cm^{-1}. The Electronic reflectance spectra of all the complexes were recorded at room temperature on a Perkin Elmer UV/Vis spectrometer in the range 400 – 190 nm (ultraviolet) and 900 – 400 nm (visible).

2.3. Corrosion Studies

The corrosion inhibition study of the azomethine ligand was carried out using mild metal steel in acidic medium under different temperature ranges and time. The steels were bought from mile 3 market and cut to 4 x 4 dimension. The steels were abraded using emery papers, washed with soap solution, rinsed in distilled water, ethanol and acetone and allowed to dry properly. After proper drying, the steels/coupons were measured to know their masses before they were put into the blank and inhibitor samples of different concentrations and then transferred into the water bath. Three different concentrations (500 ppm, 300 ppm and 100 ppm.) were used in this study. The experiment was carried out at different temperature and time (100 °C for 3 and 1 h, 50 °C for 24 and 12 h and 30 °C for 6 h) using a thermostat water bath. The masses of the coupons before and after immersion were computed and the weight loss, corrosion rate and percentage inhibition determined using the following expressions below.

$$\Delta W = m1 - m2 \quad (1) \qquad CR = \Delta W \quad (2)$$

at

$$\theta = CRa - CRp \quad (3) \qquad \%IE = \theta\, x\, 100 \quad (4)$$

CRa

Where; ΔW = Weight loss or change in weight; m1 = Initial mass before corrosion; m2 = Final mass after corrosion.

A = Sample area; CR = Corrosion rate; t = Indicates time of exposure; θ = Surface coverage; CRa = Corrosion rate in the absence of inhibitor; CRp = Corrosion rate in the presence of inhibitor; %IE =Percentage inhibition efficiency.

2.4. Antimicrobial Studies

Antimicrobial activity of the synthesized ligand and its metal(II) complexes (Mn(II), Fe(II), Co(II), Ni(II), Cu(II), and Zn(II)) was carried in-vitro by the agar diffusion technique using the bacterial *Staphylococcus aureus*, *Bacillus cereus*, *Pseudomonas aeruginosa*, *Proteus mirabilis*, *Salmonella typhi* and *Klebsiella pneumoniae* and fungal *Aspergillus niger*, *Aspergillus flaus*, and *Rhizopus stalonfer*, C_2H_6OS was used as a diluent for the compounds as well as a negative control and miconazole served as fungal positive control and Streptomycin served as bacterial positive control. A sterile cork borer of 8 mm was used to bore wells on the agar plates [14]. In each well, 80 uL of the compound was added through the aid of a micro syringe, resulting into 80 µg per well. The inoculated plates were incubated at 37°C for 18-24 h (bacteria) and 30°C for 48 h (fungi) and the diameters of inhibition zones were measured (in mm). The antimicrobial tests were carried out in duplicates and the mean activity determined. The results are recorded in Table 5.

2.5. Synthesis of the HL Ligand and its M^{2+} Complexes

2.5.1. Synthesis of |HL

About 7g of 2-hydroxyl-1-naphthaldehyde was weighed and transferred into a quick fit flask; 30mL of C_2H_5OH was added. The resultant solution was stirred for 15 mins using a magnetic stirrer/hot plate at a temperature range of 45°C -60°C to achieve homogeneity. Thereafter, 4.5g of the amine compound (4-fluoro-aniline) was measured and added to the solution followed by an addition of 30mL C_2H_5OH. The resultant solution which is shown in fig 1 below, was allowed to stir for about 5 mins followed by the addition of drops of acetic acid which served as a catalyst. The reagents were refluxed in equimolar amounts for six hours, the mixture was filtered under gravity, dried, carefully transferred into a sample bottle and placed in a desiccator.

Reaction between 2-hydroxyl-1-naphthaldehyde and 4-fluoroaniline is shown below:

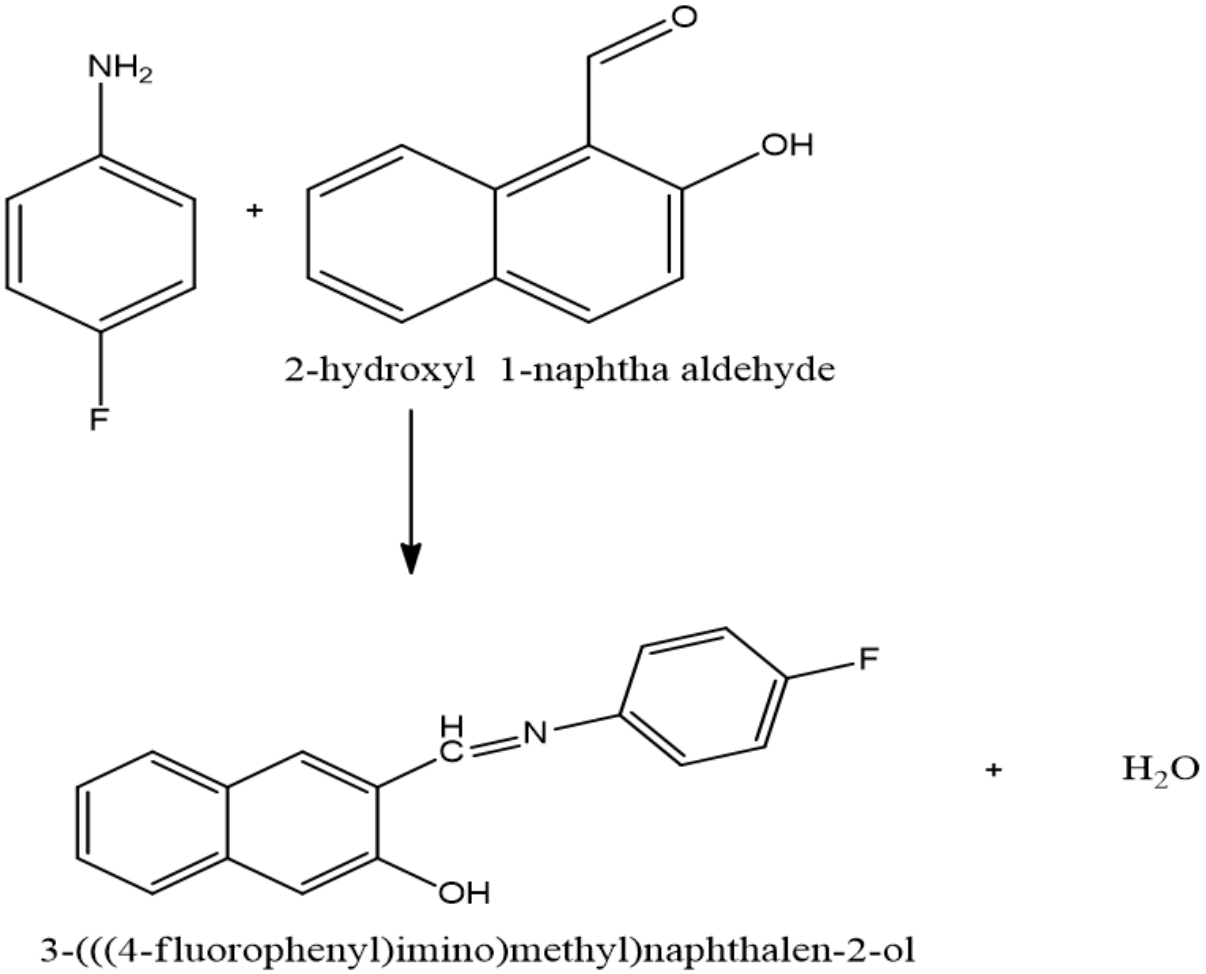

Figure 1. illustrates the reaction between 2-hydroxyl—1-naphthaldehyde with 4-fluoro aniline to give the ligand(HL).

2.5.2. Synthesis of Metal (II) Complex

Approximately 0.5 g of HL was dissolved in 20 mL distilled ethanol, stirred on a magnetic stirrer until homogenous solution was obtained. Separate solutions of 0.231 g of manganese (II)acetatetetrahydrate, 0.262 g of iron(II) tetraoxosulphate(VI) heptahydrate, 0.161 g of the cobalt(II) chloride hexahydrate, 0.231 g of nickel(II) acetate tetrahydrate, 0.225 g of copper(II) acetate dihydrate and 0.207 g of zinc(II) acetate dihydrate in 10 mL ethanol were added to the ligand solution, followed by the addition of 8 drops of triethylamine. Each resulting

mixture was allowed to reflux for 6 h during which a colour change and precipitation was observed. The products were left to cool to room temperature, and were filtered, and dried

3. RESULTS AND DISCUSSION

3.1. Analytical Studies

The azomethine chelator as well as the complexes had good yields ranging from 39.09% to 136.45%. Loss of product during purification or side reactions that divert reactants away from forming the desired product are some of the factors leading to a less than/ above a 100% in the yield composition. From stoichiometric point of view, the ligand reacted with the metals in 2:1 molar ratio. The Schiff base ligand (HL) melted in the range 160 – 165 °C whereas its metal complexes all melted in the range 125 – 285 °C and above. No metal complex had the same melting point as the azomethine based chelator thereby confirming the formation of new compounds (metal complexes) [15].

Table 1 presents an Analytical table for the ligand (HL) and its M2+ complexes.

Table 1. Analytical table for the ligand (HL) and its M2+ complexes.

Compound	MW	Shade	MPT(°C)	Yield%
$C_{17}H_{12}OFN$	265	Yellow	160-165	70.25
$Mn(C_{34}H_{24}OFN)$	584.94	Army green	125-130	39.09
$Fe(C_{34}H_{24}OFN)$	585.84	Umber brown	260-265	136.45
$Co(C_{34}H_{24}OFN)$	588.93	Dark red	185-190	51.73
$Ni(C_{34}H_{24}OFN)$	588.69	Olive green	280-285	51.63
$Cu(C_{34}H_{24}OFN)$	593.55	Siena brown	260-263	35.38
$Zn(C_{34}H_{24}OFN)$	595.38	Taupe brown	240-245	55.64

Note: MW: Molecular weight.
MPT: Melting point.

3.2. Solubility data for HL Ligand and its Metal(II) Complexes in Organic Solvents

A solubility assessment was conducted for the Hl ligand and its M^{2+} complexes across seven organic solvents at room temperature. The results indicated that both the ligand and many of its metal complexes exhibited a favorable solubility profile in C_2H_6OS, and C_3H_7NO [15]. However, the Fe^{2+} complex exhibited only limited solubility in theses solvents. In contrast, the Zn(II) and Cu(II) complexes were completely soluble in both C_2H_6OS and CH_3Cl. Both the ligand and its divalent metal complexes showed insolubility in water, suggesting their hydrophobic nature and minimal interaction with polar solvents.

3.3. Infrared Spectroscopy

The IR spectrum gives significant information about the nature of functional groups involved in coordination, mostly in synthesized organic compounds. The infrared study of the ligand, HL and its divalent copper, zinc, manganese, cobalt, nickel and iron complexes has been reported. The assignments of spectral bands were made by comparing the spectra of the synthesized compounds with reported literature on similar researches [11, 16]. In the HL ligand, the presence of a strong band observed at 3655cm^{-1} was assigned to ν(O-H) [14]. The comparative analysis of the spectrum of ligand HL revealed that the absorption band characteristic of C=N stretching vibration shifted towards higher wave number from 1623 to 1632cm^{-1} in the complexes as shown in Appendixs 1-7 [17]. Furthermore, the band arising from C=C functional group was found in the ligand spectrum at 1507 [18]. The free primary NH_2 moiety converted to azomethine group was observed by the appearance of the band at 1627cm^{-1} assigned to ν(C=N) [6]. Due to the aromatic rings contained within the synthesized HL ligand, the spectrum also showed ν(C-H) stretching band at 3064cm^{-1} [14]. The intensity bands observed at 1230cm^{-1}, 1536cm^{-1},1344cm^{-1} and

2377cm^{-1} were assigned to ν(C-C), ν(C=C), ν(C-N), and ν(C-F) individually. The presence of the hydroxyl functional group of naphtha-aldehyde on the Schiff base (HL) was confirmed by the band at 3655 cm^{-1}. An amine ν(C=N) band appeared at 1622cm^{-1}stretching vibration signifying the formation of the of Fe^{2+} complex as shown in appendix 3 [10]. As a result of the methyl group attached to the moiety of the synthesized ligand, the stretching vibration at 2972cm^{-1} was assigned to ν(C-H) [19].

Further conclusive evidence of coordination of the Schiff base with the metal ion was shown by the appearance of M-O and M-N stretching within the range of 518-563 cm^{-1} and 661cm^{-1} -659 cm^{-1} respectively.

Table 2 presents an Infrared data of the synthesized compound.

Table 2. Infrared data of the synthesized compound.

Compound	C=N	OH	C-H	C=C	C-F	C-C	C-N	M-N	M-O
HL	1623	3655	2374	1507	1230	1344	-	-	-
MnL_2	1627	3629	2345	-	-	-	-	659	563
FeL_2	1622	3630	2364	1538	-	1453	1398	-	-
CoL_2	1621	3435	-	1536	-	1387		532	-
NiL_2	1635	3453	-	1537	1229	1363		661	518
CuL_2	1622	3428	2345	1502		1432	-	501	-
ZnL_2	1632	3398	-	1541	-	1223	-	-	-

3.4. Electronic Spectroscopy

The ligand HL showed prominent absorption bands due to π-π* transitions at high wavenumbers (39,600 and 39,062 cm^{-1}) and n-π* transitions (31,847, 30,612, 29,252, and 25,000 cm^{-1}). These transitions are typical for conjugated systems with aromatic rings and non-bonding electron pairs, which promote both π-π* and n-π* transitions [20]. Additional bands at 15385, 14667, and 13115 cm^{-1} suggest intramolecular charge transfer within HL, particularly associated with the naphthalene and imine moieties, consistent with similar Schiff base ligands [21]. The CoL_2 complex displayed several absorption bands (37,594, 32,051, 30,120 cm^{-1}) due to π-π* and n-π* ligand-centered transitions. The lower-energy bands at 16,949, 15,401, 14,667, and 13,115 cm^{-1} corresponds to *d-d* transitions of $^4T_{1g} \rightarrow {}^4A_{2g}$, suggesting an octahedral geometry around Co(II). This high-spin d^7 system is consistent with an octahedral coordination, where $^4T_{1g}$ and $^4A_{2g}$ states indicate transitions within a high-spin Co(II) complex [22]. The MnL_2 complex showed high-energy π-π* and n-π* transitions at 39,600, 38,710, and 31,847 cm^{-1}, as well as a metal-ligand charge transfer (M-LCT) band at 25,000 cm^{-1}. The latter implies interaction between Mn and the ligand through coordination bonds. Additional bands at 16,611, 15,674, and 14,641 cm^{-1}, attributed to $^6A_{1g} \rightarrow {}^4T_{1g}(G)$, $^6A_{1g} \rightarrow {}^4T_{1g}$, and $^6A_{1g} \rightarrow {}^4T_{2g}(G)$ transitions, confirm an octahedral geometry around Mn(II) (Clarke et al., 2018). The FeL_2 complex showed distinct n-π* and π-π* transitions in the UV region, with additional bands at 27,322, 26,739, and 24,874 cm^{-1} attributed to charge transfer transitions. Lower-energy bands at 15,936 and 14,667 cm^{-1} corresponds to $^5T_{2g} \rightarrow {}^5E_g$ transitions, consistent with Fe(II) in an octahedral environment. The Jahn-Teller distortion was indicated by broad absorption bands at 16,077 and 14,684 cm^{-1} [23]. The NiL_2 complex displayed transitions at 33,333, 29,252, and 25,381 cm^{-1} due to π-π* and n-π* ligand-centered transitions, while lower-energy bands at 15,573 and 14,706 cm^{-1} were assigned to $^3A_{2g} \rightarrow {}^3T_{1g}(F)$ transitions. These are characteristic of Ni(II) complexes in an octahedral field, where an octahedral coordination stabilizes the d^8 configuration and produces visible d-d transitions [24]. The CuL_2 complex exhibits a broad band around 13,123 cm^{-1} assigned to the $^2E_g \rightarrow {}^2T_{2g}$ transition, typical of Cu(II) in an octahedral field with Jahn-Teller distortion [25]. The broadening and asymmetry of this band suggest a distortion in the Cu(II) coordination environment, likely indicating an elongated octahedral structure. The CuL_2 complex also showed high-energy π-π* and n-π* transitions (38,462 and 33,557 cm^{-1}). The ZnL_2 complex exhibited absorption bands at 28,462 and 30,120 cm^{-1},

corresponding to π-π* and n-π* transitions within the ligand. Zn(II), being d^{10}, lacks d-d transitions, which is typical for Zn(II) complexes [26]. This electronic behavior aligns with the closed d^{i0} configuration of Zn(II) in a stable octahedral geometry Table 3 presents Electronic spectral data.

Table 3. Electronic spectral data.

Compounds	Absorption band (cm^{-1})	Band assessment	Geometry
HL	39600, 39062 31847, 30612 29252, 25000, 15385, 14667,13115	π-π* n-π* $^1A_{1g}(D) \rightarrow {}^1A_{2g}(D)$ $^2B_{1g} \rightarrow {}^2A_{1g}$	Octahedral
CoL_2	37594, 32051, 30120, 16949, 15401, 14667, 13115, 12804	π-π* n-π* $^4T_{1g} \rightarrow {}^4A_{2g}$	Octahedral
MnL_2	39600, 38710, 31847, 29940, 27778, 26739, 25641, 15525, 14706, 12958, 12689	π-π* n-π* $^6A_{1g} \rightarrow {}^4T_{1g}$ M-LCT	
FeL_2	37594, 33780, 30303, 27322, 26739, 24874, 23529, 22522, 21832, 15936, 14667, 13115	n-π* π-π* $^5T_{2g} \rightarrow {}^5E_g$	Octahedral
NiL_2	33333, 29252, 28249, 25381, 15573, 14706	π-π* n-π* $^3A_{2g} \rightarrow {}^3T_{2g}$	Octahedral
CuL_2	38462, 33557, 25000, 15385, 14605, 13115	π-π* n-π* $^2E_g \rightarrow {}^2T_{2g}$	Octahedral
ZnL_2	28462, 32680, 31250, 30120, 28736	π-π* n-π* $^1A_{1g(D)} \rightarrow {}^1A_{2g(D)}$ $^4A_{2g} \rightarrow {}^2A_{1g}$	Octahedral

Note: The (*) indicates an antibonding molecular orbital. During electronic transitions, it represents the excited state where an electron moves from a lower energy orbital to a higher energy aantibonding state.

4. APPLIED STUDIES

4.1. Corrosion Inhibition Studies of the HL Ligand

Corrosion inhibition of mild steel immersed in 100-500ppm of 1M-HCl solution at varied temperature and time attained from weight loss (WL) measurements. The impact of the ligand on acid corrosion of mild steel in 1M HCl, gravimetric assessments of mild steel was carried out in the presence of 100, 300, and 500ppm of the ligand in a uniform solution at room temperature. A 100ppm blank solution was used as a control. The percentage inhibition efficiency(IE) and corrosion rate (CR) calculated from weight loss results for 1, 3, 12 and 24 hours are given.

It could be observed from the information that the ligand ($C_{17}H_{12}ONF$) confirmed substantial corrosion inhibition behaviour in opposition to corrosion of mild steel in a 1M HCl solution. What propelled the inhibition performance of the $C_{17}H_{12}ONF$ towards the mild steel could be due to the coordination through the donor acceptor interplay among the unshared electron pairs of donor atoms of the ligand [27]. The calculated values of CR, θ and IE from gravimetric evaluation at different concentrations of the studied inhibitor at different temperatures and times are summarized in Tables 4a-f The results indicated that corrosion rate decreases with increase in concentration. The decrease is as a result of inhibitive effect of the inhibitor concentration. It is visible from Table 4d hat inhibition efficiency arose with increased inhibitor concentration yielding a value of 68.08, 7.54, 84.10 and 91.61 percent for 1, 3, 12 and 24 hours separately. This is attributed to the adsorption of $C_{17}H_{12}ONF$ on the mild

steel surface through bonding free electron pairs of N-, F- and O- species as well as pi-electrons of the cyclic rings joining alongside to the imine moiety.

The corrosion rate at different concentrations was affected by time of the immersion of steel in 1M HCl. The plot of inhibition efficiency against concentration is showed in Figures 1 to Figure 6. The result showed that increased in inhibition efficiency was consistence with increase in concentration indicating that $C_{17}H_{12}ONF$ performed through association of a resistance layer and the corrosive medium by its adsorption on the mild steel surface. The inhibitory proficiency was enhanced with improved concentration of $C_{17}H_{12}ONF$. This indicates corrosion inhibition is an end result of adsorption of inhibitor on the metal surface and the ligand acts as adsorption inhibitor. Better inhibition efficiency at higher concentration could be ascribed to greater coverage of metal with inhibitor molecule [28-30].

Table 4a. Corrosion inhibition studies at 1hour for 373k.

Compound	Conc.	CR	%IE	θ	ΔW
$C_{17}H_{12}ONF$	Blank	0.003457	-	-	0.055315
	100	0.001934	44.06	0.440676	0.0309375
	300	0.001660	52.04	0.503742	0.06565
	500	0.001117	68.08	0.680791	0.017875

Table 4b. Corrosion inhibition studies at 3 hours for 373k.

Compound	Conc.	CR	%IE	θ	ΔW
$C_{17}H_{12}ONF$	Blank	0.00381	-	-	0.1575
	100	0.00316	1.98	0.198	0.154375
	300	0.00315	4.76	0.047619	0.15
	500	0.0030338	7.54	0.075397	0.14565

Table 4c. Corrosion inhibition studies at 12 hours for 323k.

Compound	Conc.	CR	%IE	θ	ΔW
$C_{17}H_{12}ONF$	Blank	0.00015	-	-	0.0415
	100	0.0000638	70.30	0.703031	0.01225
	300	0.0000374	82.60	0.82605	0.007188
	500	0.00003418	84.10	0.84103	0.006565

Table 4d. Corrosion inhibition studies at 24 hours for 323k.

Compound	Conc.	CR	%IE	θ	ΔW
$C_{17}H_{12}ONF$	Blank	0.00027728	-	-	0.1064375
	100	0.00009798	64.66	0.64663	0.037625
	300	0.000034017	87.73	0.877319	0.013063
	500	0.000023275	91.61	0.9160596	0.008937

Table 4e. Corrosion inhibition studies at 1 hour and 3 hours for 373k.

Compound	Concentration	1 hour/ IE(%)	3hours/ IE(%)
373K	100	44.06	1.98
	300	52.04	1.95
	500	68.08	7.53

Table 4f. Corrosion inhibition studies at 12 hours and 24 hours for 323k.

Compound	Concentration	12hours/ IE(%)	24hours/ IE(%)
323K	100	70.30	64.66
	300	82.60	87.73
	500	84.10	91.61

Figure 2 Illustrates the variation of corrosion rate (a) and inhibition efficiency (b) against concentration of $C_{17}H_{12}ONF$ at 373k and 1 hour.

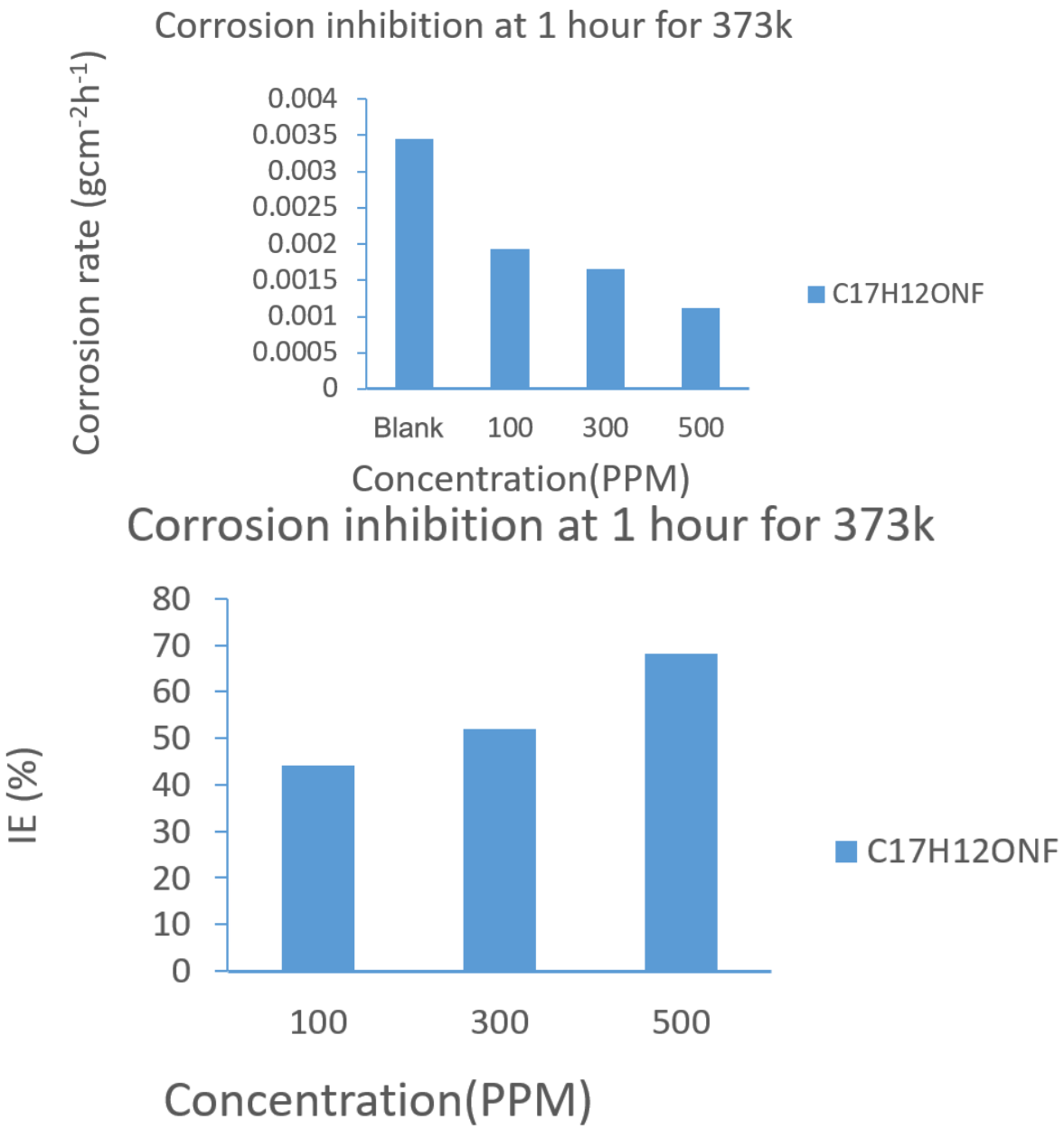

Figure 2. Variation of corrosion rate (a) and inhibition efficiency (b) against concentration of $C_{17}H_{12}ONF$ at 373k and 1 hour.

Figure 3 illustrates the variation of corrosion rate (a) and inhibition efficiency (b) against concentration of $C_{17}H_{12}ONF$ at 373k and 3 hour.

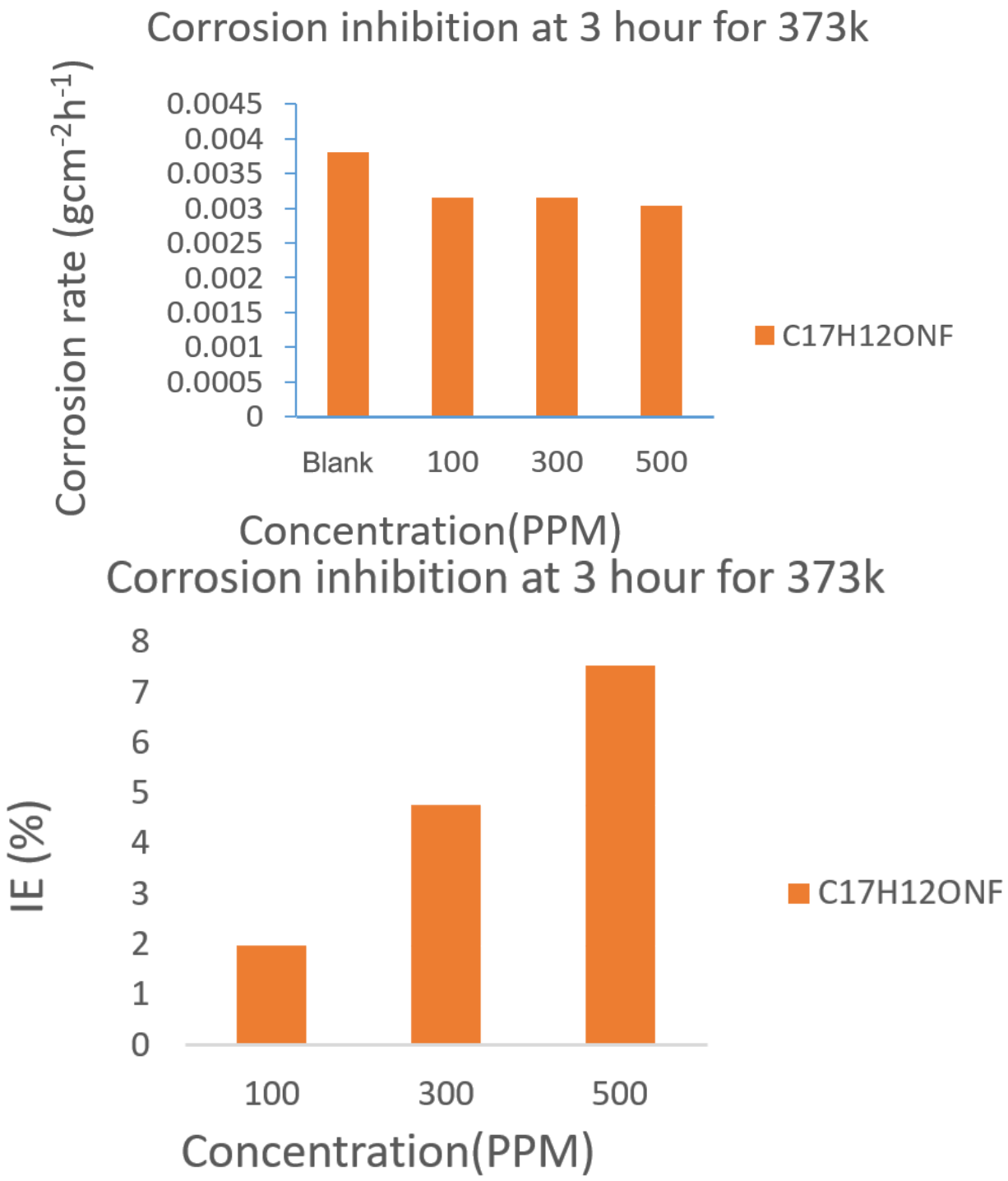

Figure 3. Variation of corrosion rate (a) and inhibition efficiency (b) against concentration of $C_{17}H_{12}ONF$ at 373k and 3 hour.

Figure 4 illustartes the variation of corrosion rate (a) and inhibition efficiency (b) against concentration of $C_{17}H_{12}ONF$ at 323k and 12 hour.

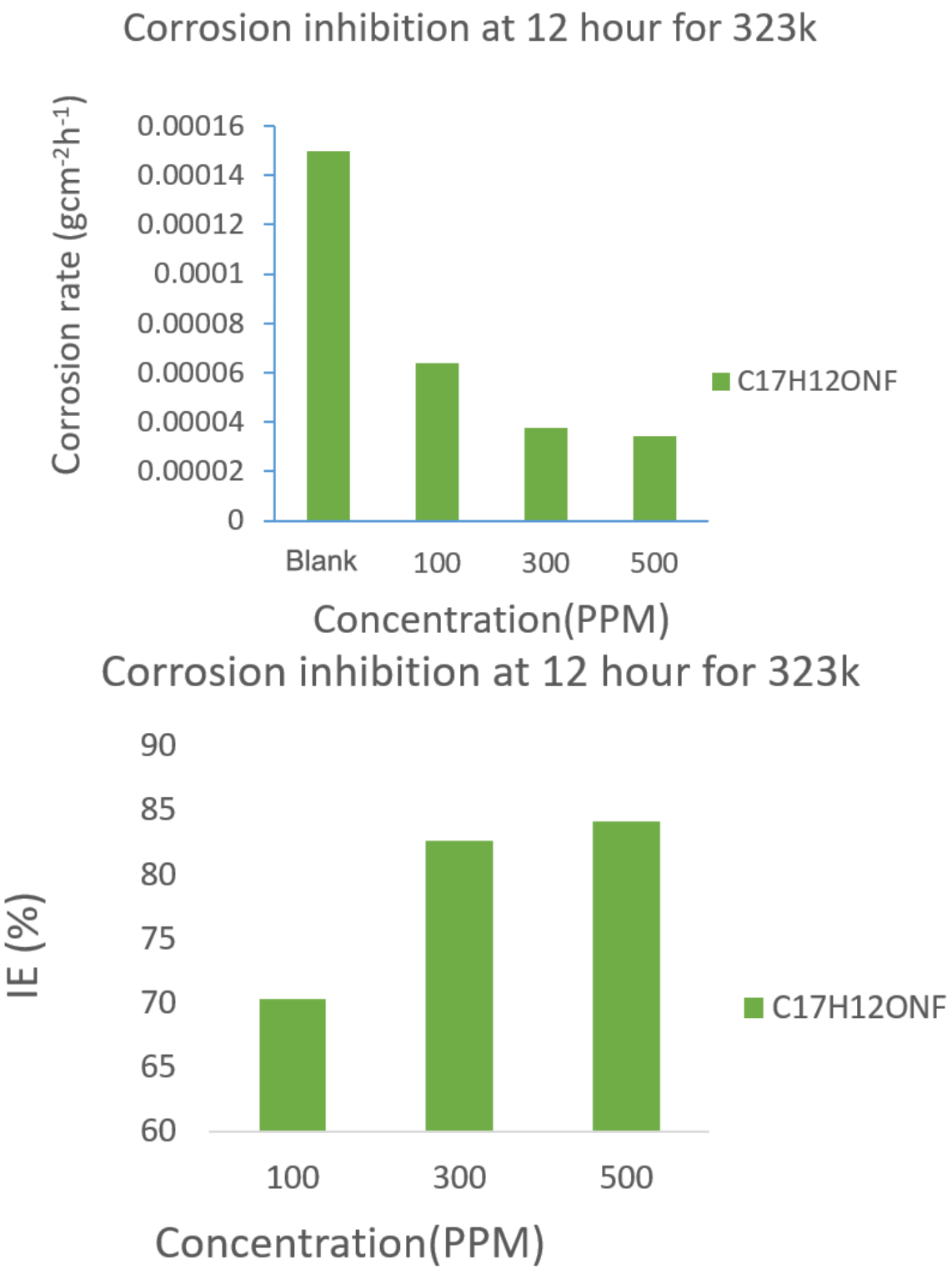

Figure 4. Variation of corrosion rate (a) and inhibition efficiency (b) against concentration of $C_{17}H_{12}ONF$ at 323k and 12 hour.

Figure 5 illustrates the variation of corrosion rate (a) and inhibition efficiency (b) against concentration of $C_{17}H_{12}ONF$ at 323k and 24 hour.

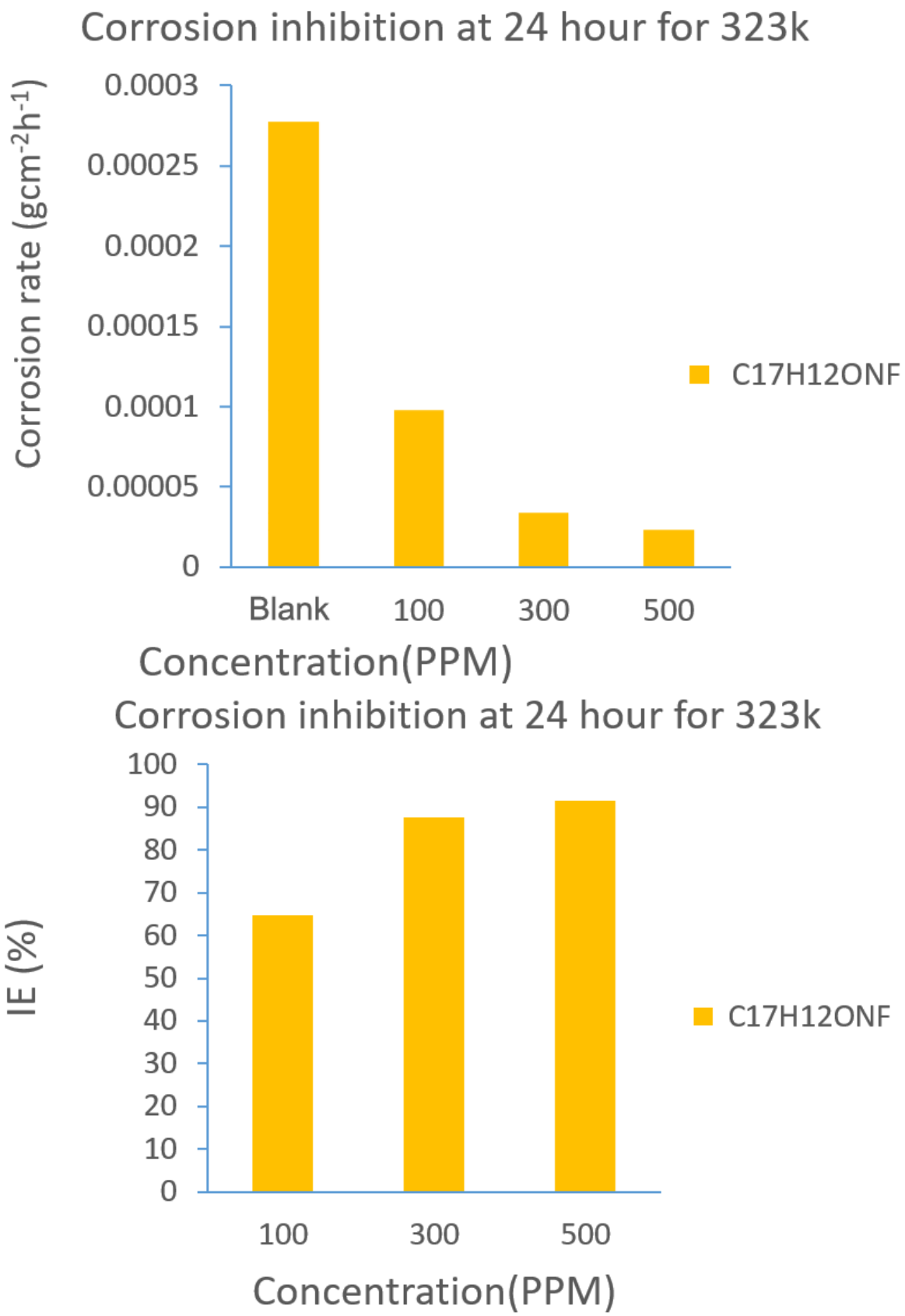

Figure 5. Variation of corrosion rate (a) and inhibition efficiency (b) against concentration of $C_{17}H_{12}ONF$ at 323k and 24 hour.

Figure 6 illustrates the variation of inhibition efficiency at 1 hour and 3 hours against concentration of $C_{17}H_{12}ONF$ at 373k.

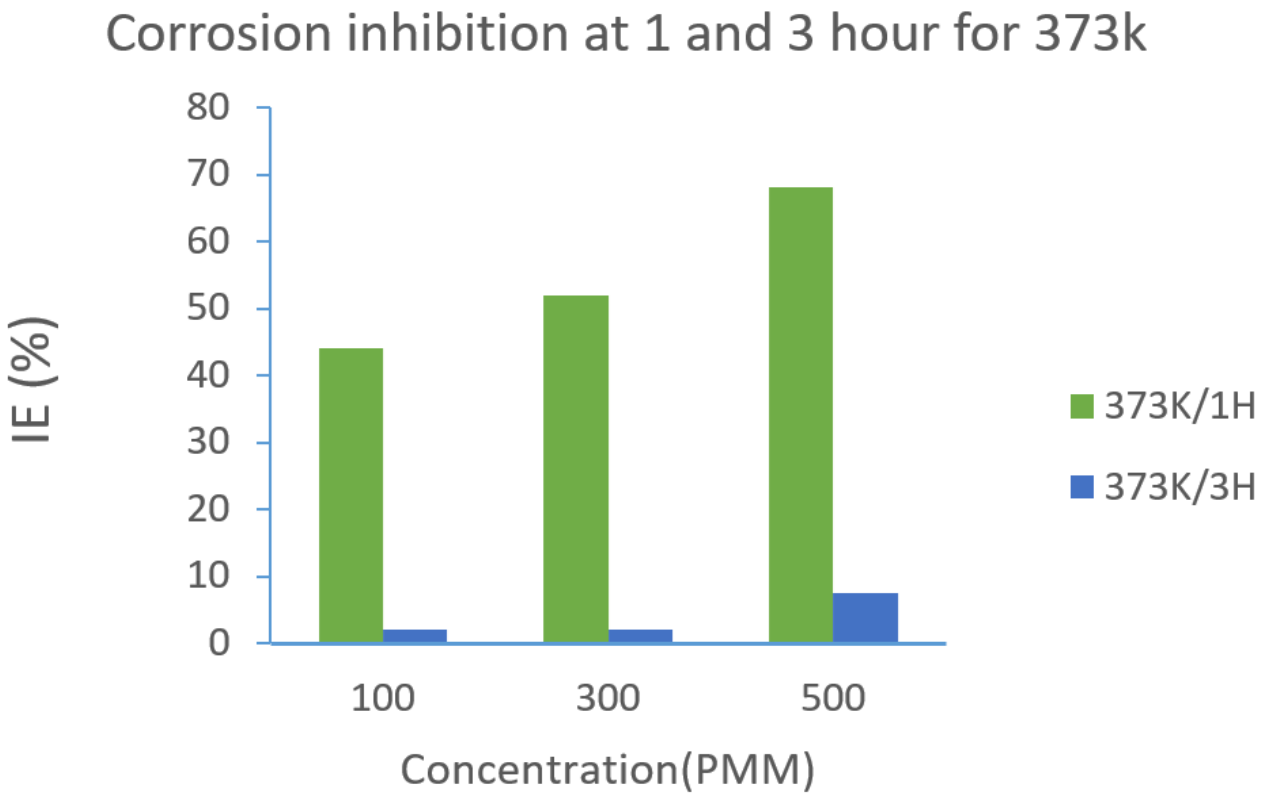

Figure 6. Variation of inhibition efficiency at 1 hour and 3 hours against concentration of $C_{17}H_{12}ONF$ at 373k.

Figure 7 Illustrates the variation of inhibition efficiency at 12 hours and 24 hours against concentration of $C_{17}H_{12}ONF$ at 323k.

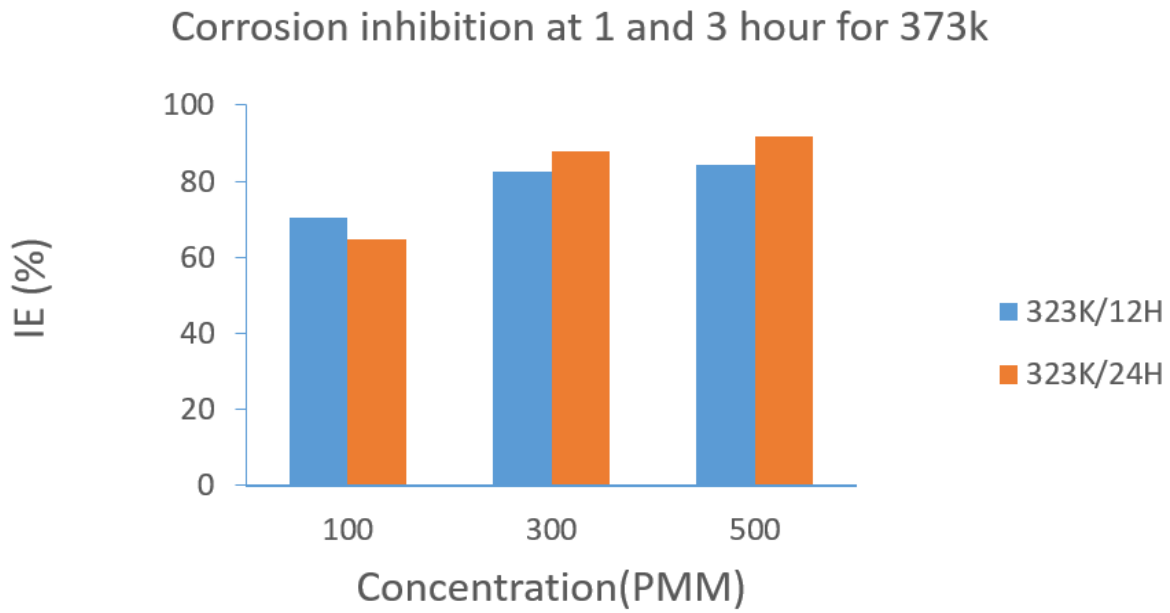

Figure 7. Variation of inhibition efficiency at 12 hours and 24 hours against concentration of $C_{17}H_{12}ONF$ at 323k.

Note: PPM: parts per million.

4.2. Antimicrobial Studies

The HL ligand and their metal complexes were apprised against nine antimicrobial strains *(staphylococcus aureus, pseudomonas aeruginosa, klebsilla oxytoca, salmonella T, proteus mirabilis, bacillus cereus)* for antimicrobial activity.

The inhibition growth zone diameter was used as criteria to measure the antibacterial activities of the metal complexes presented in the table. It was observed that the complexes showed higher activities than the free ligands. The anti-microbial results presented in the table indicates that all the tested complexes were active against all the bacteria species except *Proteus mirabilis* which failed to show any action on some metal (II) complexes.

The heteroleptic bivalent complexes displayed better inhibitory effects against the bacterial strains than the parent imine chelator. The Co^{2+} chelate was active against all microbial species except *R. Stolonifera K. pneumonia, P. mirabilis, S. typhi* zone. The Cu^{2+} complex showed high activity against *Bicilus cereus* and moderate activity against *S. aueus, P. aeruginosa, K. pneumonia* and absent activity against *proteus mirabilis.* The Ni^{2+} complexes displayed moderate activity against *Staphylococcus and Bacillus cereus.* and have no activity against *P. mirabilis, k. pneumonia, P. aeruginosa, and Salmoneli typhi.* The Zn^{2+} complex showed moderate activity against *S. typhi* and no activity against *proteus mirabilis, K. pneumonia* and *P. aeruginosa.* The Co^{2+} complex demonstrated no activity against *K .pneumonia, proteus mirabiliss, S.typhi.*

Furthermore, the Ni^{2+} complex demonstrated activity against all the bacteria used for the testing except for *K. pneumonia, P. mirabilis, P. aeruginosa and S. typhi* respectively. The enhanced anti-bacteriological action of the M^{2+} complexes over their chelator agent might be expound on the basis of overtone concept [14]. The former proposes that the lipid membrane enveloping the cell allows the passage of only lipid soluble materials due to hydrophobicity which is a considerable factor that controls the antimicrobial action, whereas the latter holds that the polarity of the M^{2+}ion will be minimized to a greater extent due to overlap of the chelator's orbital and partial sharing of the positive charge(s) of the metal ions with donor groups [31].

Table 5. Presents the Antimicrobial activity of the metal (II) complexes.

Compound	A. Niger	A. Flavus	R. Stolonifer	K. Pneumonia	P. Mirabilis	P. aeruginosa	S. Typhi	S. Aureus	B. cereus
HL37	23.5±0.5	17.0±1.0	14.0±0.0	4.0±0.0	0.0±0.0	8.0±0.0	0.0±0.0	0.0±0.0	0.0±0.0
Mn($C_{34}H_{24}OFN$)	15.0±1.4	15.0±1.4	3.0±1.4	0.0±0.0	1.0±1.4	0.0±0.0	21.0±1.4	0.0±0.0	2.0±0.0
Ni($C_{34}H_{24}OFN$)	13.0±1.4	11.0±1.4	5.0±1.4	0.0±0.0	0.0±0.0	0.0±0.0	0.0±0.0	4.0±0.0	4.0±0.0
Co($C_{34}H_{24}OFN$)	6.0±0.0	14.0±0.0	0.0±0.0	0.0±0.0	0.0±0.0	2.0±0.0	0.0±0.0	9.0±1.4	1.0±1.4
Fe($C_{34}H_{24}OFN$)	14.0±0.0	19.0±1.4	6.0±0.0	3.0±4.2	2.0±0.0	0.0±0.0	0.0±0.0	1.0±1.4	11.5±0.7
Cu($C_{34}H_{24}OFN$)	12.5±0.7	14.5±0.7	8.5±0.7	2.0±2.8	0.0±0.0	4.0±0.0	4.0±0.0	6.5±0.7	11.0±1.4
Zn($C_{34}H_{24}OFN$)	7.5±0.7	16.0±0.0	5.0±1.4	0.0±0.0	0.0±0.0	0.0±0.0	2.0±0.0	15.5±0.7	20.0±0.0

5. CONCLUSION

The HL was synthesized from the reaction of 4-fluoroaniline with 2-hydroxy-1-naphthaldehyde. Mn(II), Fe(II), Co(II), Ni(II), Cu(II) and Zn(II) complexes were prepared from 2:1 stoichiometric reaction of the ligand and metal salts. The results obtained from the analytical and spectra data were used to characterize the ligand and the complexes in order to discover the components and properties of the compounds. Through the FT-IR data it was confirmed that coordination between the ligand and the metal ions took place and this coordination occurred between the metal and nitrogen as well as between the metal and oxygen donors. The electronic spectra suggested the proposed geometry for the complexes. The corrosion study validated the ligand as a good inhibitory agent. Also, the antimicrobial screening also revealed that the ligand and its metal(II) complexes had significant antifungi and antibacterial activities and so, they could be promising antibacterial and antifungal agents.

REFERENCES

[1] N. Filipović *et al.*, "Comparative study of the antimicrobial activity of selenium nanoparticles with different surface chemistry and structure," *Frontiers in Bioengineering and Biotechnology*, vol. 8, p. 624621, 2021. https://doi.org/10.3389/fbioe.2020.624621

[2] F. Fei, T. Lu, X.-T. Chen, and Z.-L. Xue, "Synthesis and structural characterization of metal complexes with macrocyclic tetracarbene ligands," *New Journal of Chemistry*, vol. 41, no. 22, pp. 13442-13453, 2017. https://doi.org/10.1039/c7nj02485a

[3] T. L. Yusuf *et al.*, "Design of new schiff-base copper (II) complexes: Synthesis, crystal structures, DFT study, and binding potency toward cytochrome P450 3A4," *ACS Omega*, vol. 6, no. 21, pp. 13704-13718, 2021.

[4] I. Ejidike and P. A. Ajibade, "Synthesis, characterization, and antioxidant properties of Schiff base complexes," *Journal of Inorganic Chemistry and Applications*, vol. 45, no. 2, pp. 202-210, 2023.

[5] O. G. Idemudia and E. C. Hosten, "Spectroscopy, crystal and molecular structures of new 4-acylpyrazolone dinitrophenylhydrazones," *Crystals*, vol. 6, no. 10, p. 127, 2016. https://doi.org/10.3390/cryst6100127

[6] K. A. Elachi, S. Hossain, M. Haque, and R. K. Mohapatra, "Synthesis, spectral and thermal characterization of Cu (II) complexes containing schiff base ligands and their antibacterial activity study," *American Journal of Materials Synthesis and Processing*, vol. 4, no. 1, pp. 43-53, 2019. https://doi.org/10.11648/j.ajmsp.20190401.16

[7] N. Kumar, S. Pratima, P. Aastha, and A. Prasad, "Synthesis and characterization of some new schiff base," *International Journal of Chemical And Pharmaceutical Sciences*, vol. 23, no. 2, pp. 231-236, 2013.

[8] S. Chigurupati, "Designing new vanillin Schiff bases and their antibacterial Studies," *Journal of Medical and Bioengineering*, vol. 4, pp. 363-366, 2015. https://doi.org/10.12720/jomb.4.5.363-366

[9] S. Mohapatra *et al.*, "Applications of Schiff bases and their metal complexes in coordination chemistry and industry," *AIP Conference Proceedings*, vol. 2142, no. 1, p. 060002, 2019.

[10] M. U. Rehman, M. Imran, M. Arif, and M. Farooq, "Synthesis, characterization and metal picrate extraction studies of salicylaldehyde derived macrocyclic schiff bases," *International Research Journal of Pure and Applied Chemistry*, vol. 4, no. 2, pp. 243-250, 2014. https://doi.org/10.9734/irjpac/2014/8147

[11] N. Ahmed, M. Riaz, A. Ahmed, and M. Bhagat, "Synthesis, characterisation, and biological evaluation of Zn (II) complex with tridentate (NNO Donor) schiff base ligand," *International Journal of Inorganic Chemistry*, vol. 2015, no. 1, p. 607178, 2015. https://doi.org/10.1155/2015/607178

[12] E. T. Obasuyi, A. I. Aigbodion, and S. Edema, "Synthesis and antimicrobial activity of some Schiff bases and their metal complexes," *International Journal of Advanced Research in Physical Science*, vol. 5, no. 10, pp. 1-8, 2018.

[13] F. Azam, A. Sultana, and S. Saeed, "Schiff bases: Versatile ligands and their metal complexes for diverse biological applications," *Journal of Molecular Structure*, vol. 1195, pp. 415-432, 2019.

[14] F. Chioma *et al.*, "Synthesis, characterization, in-vitro antimicrobial properties, molecular docking and DFT studies of 3-{(E)-[(4, 6-dimethylpyrimidin-2-yl) imino] methyl} naphthalen-2-ol and heteroleptic Mn (II), Co (II), Ni (II) and Zn (II) complexes," *Open Chemistry*, vol. 16, no. 1, pp. 184-200, 2018. https://doi.org/10.1515/chem-2018-0020

[15] M. F. Yesmin *et al.*, "Cu (II) and Ni (II) complexes of schiff base: Synthesis, characterization and antibacterial activity," *International Journal of Advanced Research in Chemical Science*, vol. 7, no. 1, pp. 9-15, 2020. https://doi.org/10.20431/2349-0403.0701002

[16] C. Festus and C. Wodi, "Corrosion inhibition; and antimicrobial studies of bivalent complexes of 1-(((5-ethoxybenzo [d] thiazol-2-yl) imino) methyl) naphthalene-2-ol chelator: Design, synthesis, and experimental characterizations," *Direct Research Journal of Chemistry and Materials Science*, vol. 8, pp. 31-43, 2021.

[17] F. S. Sani and N. Dailami, "Comparative analysis of Schiff base metal(II) complexes: Synthesis, characterization, and antimicrobial activity," *Chemical Science Journal*, vol. 6, no. 2, pp. 36-39, 2015.

[18] V. Govindaraj and S. Ramanathan, "Synthesis, spectral characterisation, electrochemical, and fluorescence studies of biologically active novel Schiff base complexes derived from E-4-(2-hydroxy-3-methoxybenzlideneamino)-N-

(pyrimidin-2-yl) benzenesulfonamide," *Turkish Journal of Chemistry*, vol. 38, no. 4, pp. 521-530, 2014. https://doi.org/10.3906/kim-1301-83

[19] A. Osowole and C. Festus, "Synthesis, characterization, antibacterial and antioxidant activities of some heteroleptic Metal (II) complexes of 3-{[-(pyrimidin-2-yl) imino] methyl} napthalen-2-ol," *Journal of Chemical, Biological and Physical Sciences*, vol. 6, no. 1, pp. 080-089, 2015.

[20] J. Smith and H. Lee, "Optical properties of conjugated Schiff base ligands in transition metal complexes," *Inorganica Chimica Acta*, vol. 444, pp. 178-185, 2016.

[21] R. Kumar, A. Singh, and M. Gupta, "Electronic spectral analysis of Schiff base ligands with transition metals," *Journal of Coordination Chemistry*, vol. 72, no. 5, pp. 789-798, 2019.

[22] R. Sharma and S. Gupta, "Electronic properties of cobalt-Schiff base complexes," *Journal of Chemical Physics*, vol. 148, no. 7, pp. 1302-1309, 2018.

[23] J. Brown and T. Nguyen, "Spectroscopic analysis of transition metal-Schiff base complexes," *Journal of Inorganic Chemistry*, vol. 60, no. 7, pp. 2244-2255, 2021.

[24] P. Chowdhury and P. Balakrishnan, "Electronic spectra and molecular modeling of nickel complexes with tetradentate ligands," *Polyhedron*, vol. 110, pp. 1-8, 2016.

[25] T. O'Brien and A. Singh, "Electronic transitions in copper complexes with bidentate ligands," *Transition Metal Chemistry*, vol. 42, no. 5, pp. 1203-1212, 2017.

[26] P. A. Larsen and A. Kumar, "Electronic spectral studies on octahedral zinc(II) complexes," *Transition Metal Chemistry*, vol. 44, no. 2, pp. 345-355, 2019.

[27] O. U. Nnenna, J. C. Onwuka, and S. A. Adebayo, "The role of coordination through donor–acceptor interplay in inhibiting mild steel corrosion," *Journal of Inorganic Chemistry*, vol. 58, no. 3, pp. 321-333, 2020.

[28] P. Singh, A. K. Singh, and V. P. Singh, "Synthesis, structural and corrosion inhibition properties of some transition metal (II) complexes with o-hydroxyacetophenone-2-thiophenoyl hydrazone," *Polyhedron*, vol. 65, pp. 73-81, 2013. https://doi.org/10.1016/j.poly.2013.08.008

[29] Y. B. Zemede, D. Nithyakalyani, and A. Kumar, "Synthesis, structural characterization,corrosion inhibition and in vitro antimicrobial studies of 2-(5-methoxy-2hydroxybenylideneamino) phenol Schiff base ligand and its transition metal complexes," *Synthesis*, vol. 6, no. 11, pp. 4569-4578, 2014.

[30] F. Chioma, J. Ayogu, and C. U. Ibeji, "Ligation actions of 2-(3-hydroxypyridin-2-ylamino) naphthalen-1, 4-dione: Synthesis, characterization, in-vitro antimicrobial screening, and computational studies," *Indian Journal of Heterocyclic Chemistry*, vol. 31, no. 1, pp. 1-13, 2021.

[31] A. A. Osowole and C. Festus, "Synthesis, characterization and antibacterial activities of some metal (II) complexes of 3-(-1-(2-pyrimidinylimino) methyl-2-napthol," *Elixir Applied Chemistry*, vol. 59, pp. 15843-15847, 2013.

APPENDICES

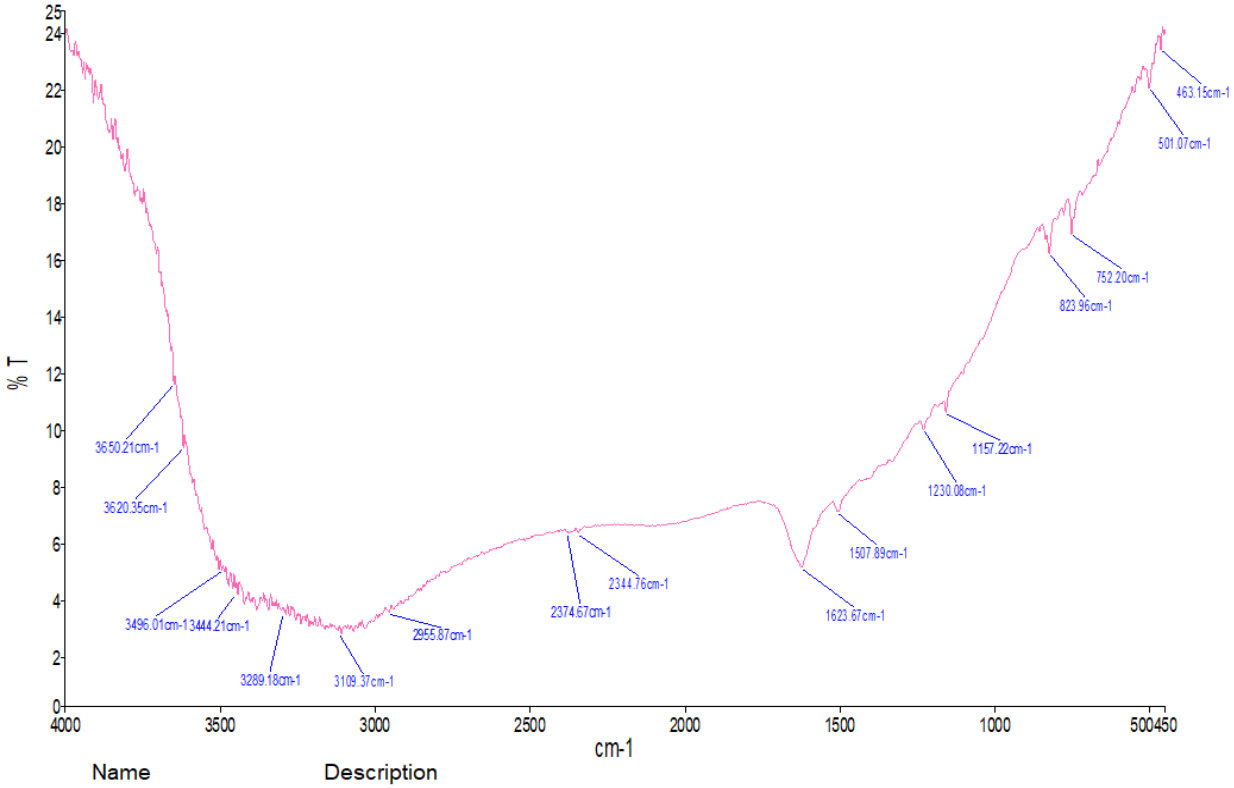

Appendix 1. Illustrates the FT-IR spectrum of Co(II) metal complexes.

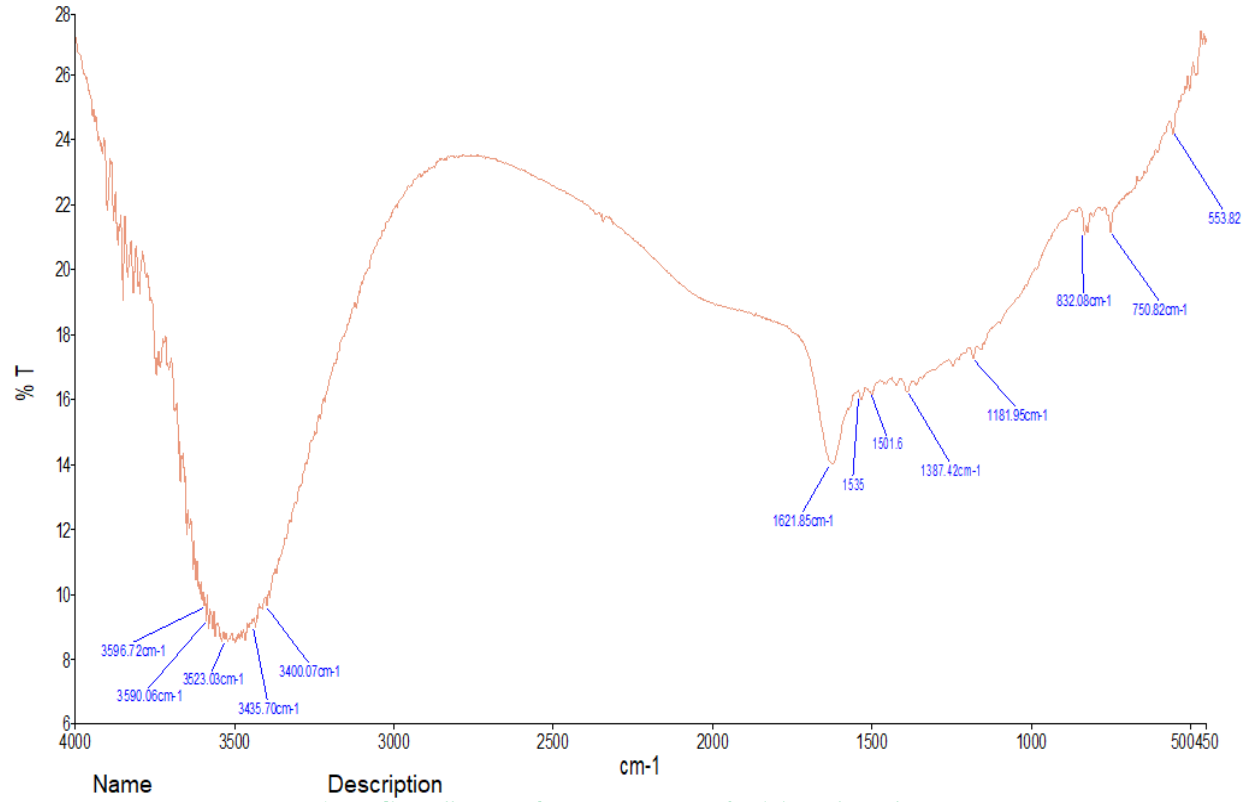

Appendix 2. Illustrates the FT-IR spectrum of Cu(II) metal complexes.

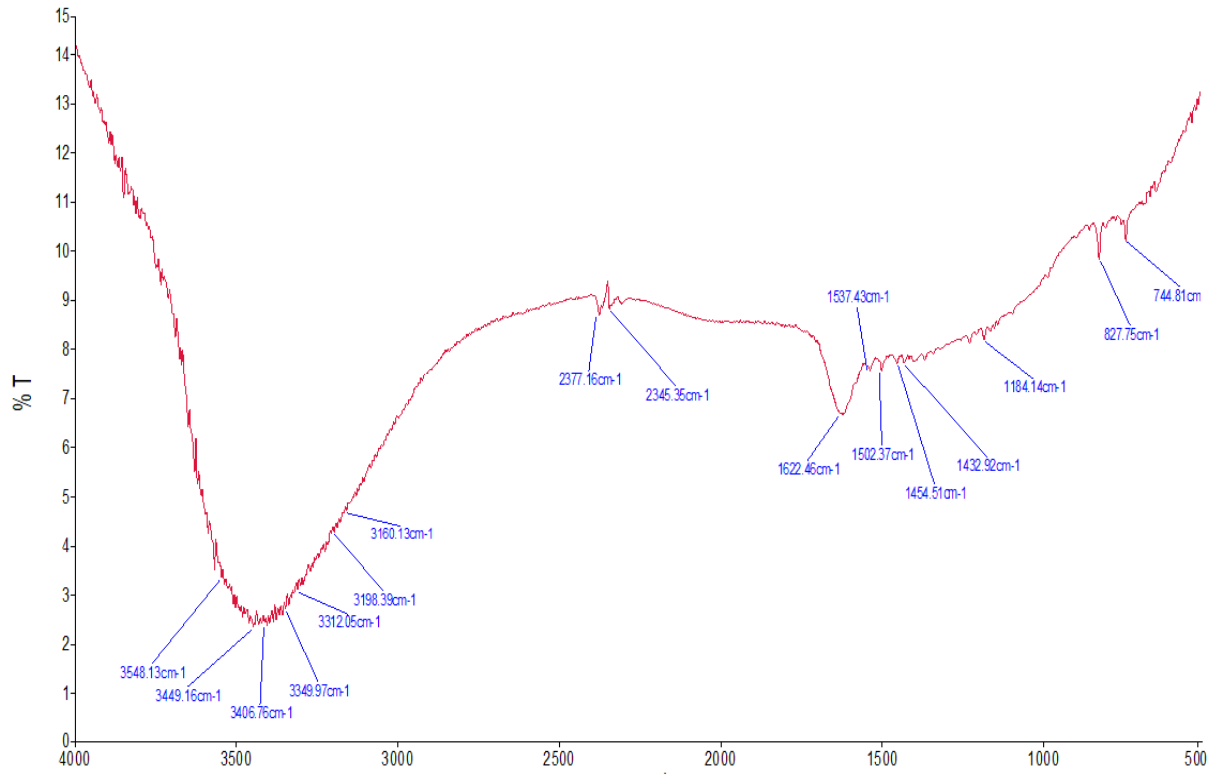

Appendix 3. Illustrates the FT-IR spectrum of Fe(II) metal complexes.

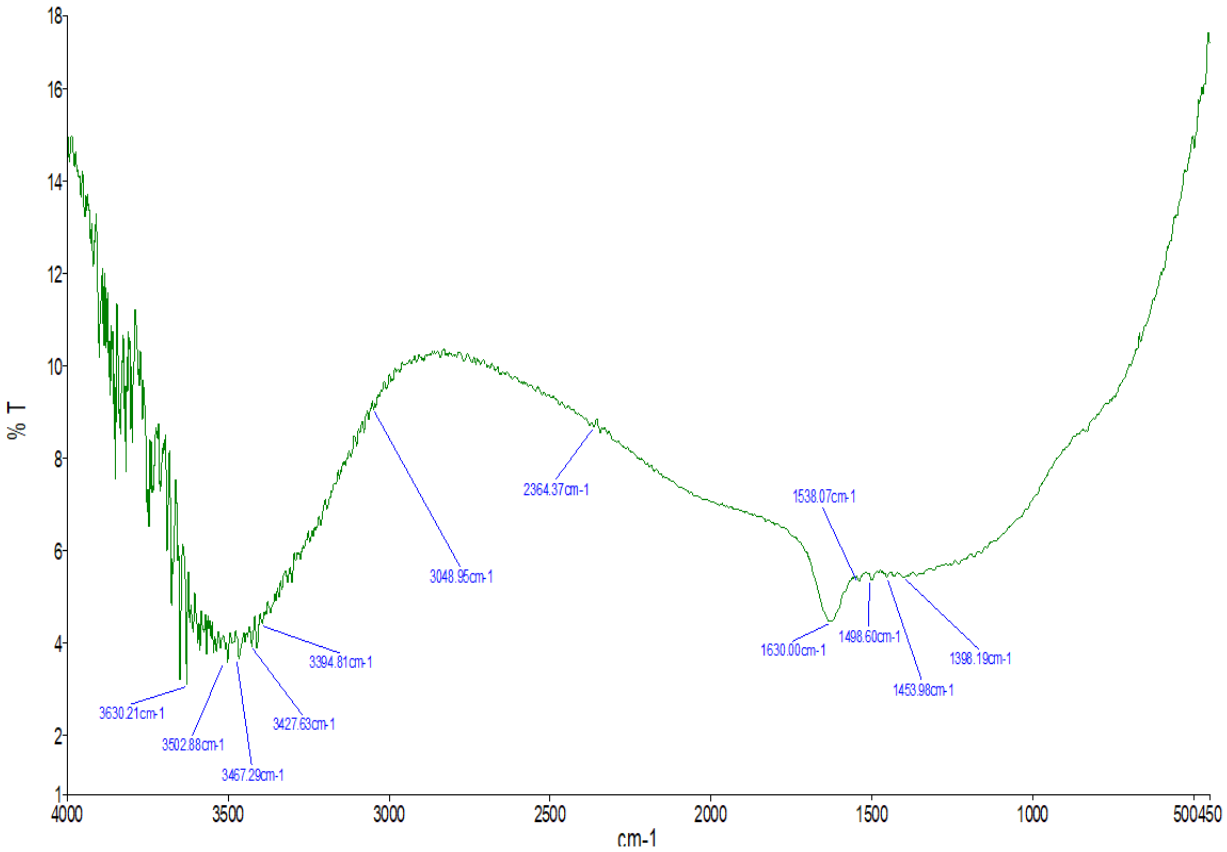

Appendix 4 Illustrates the FT-IR spectrum of Mn(II) metal complexes.

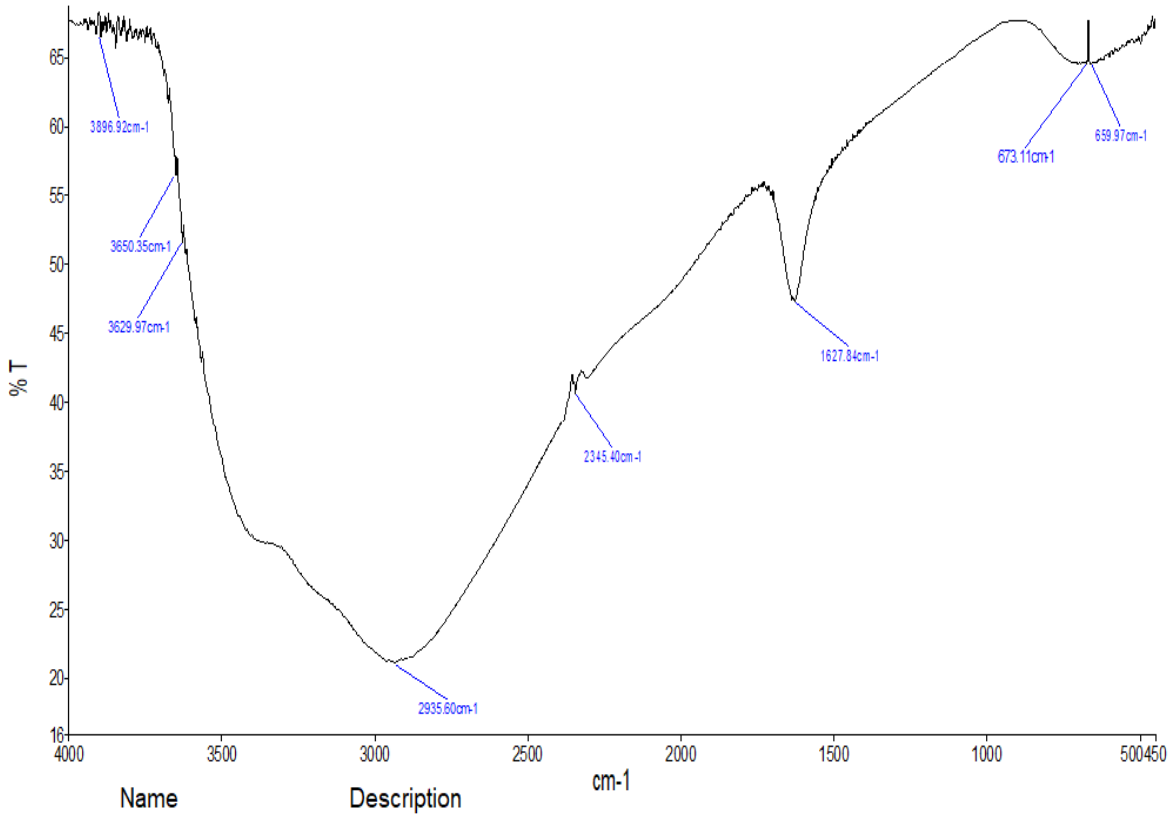

Appendix 5. Illustrates the FT-IR spectrum of Ni(II) metal complexes.

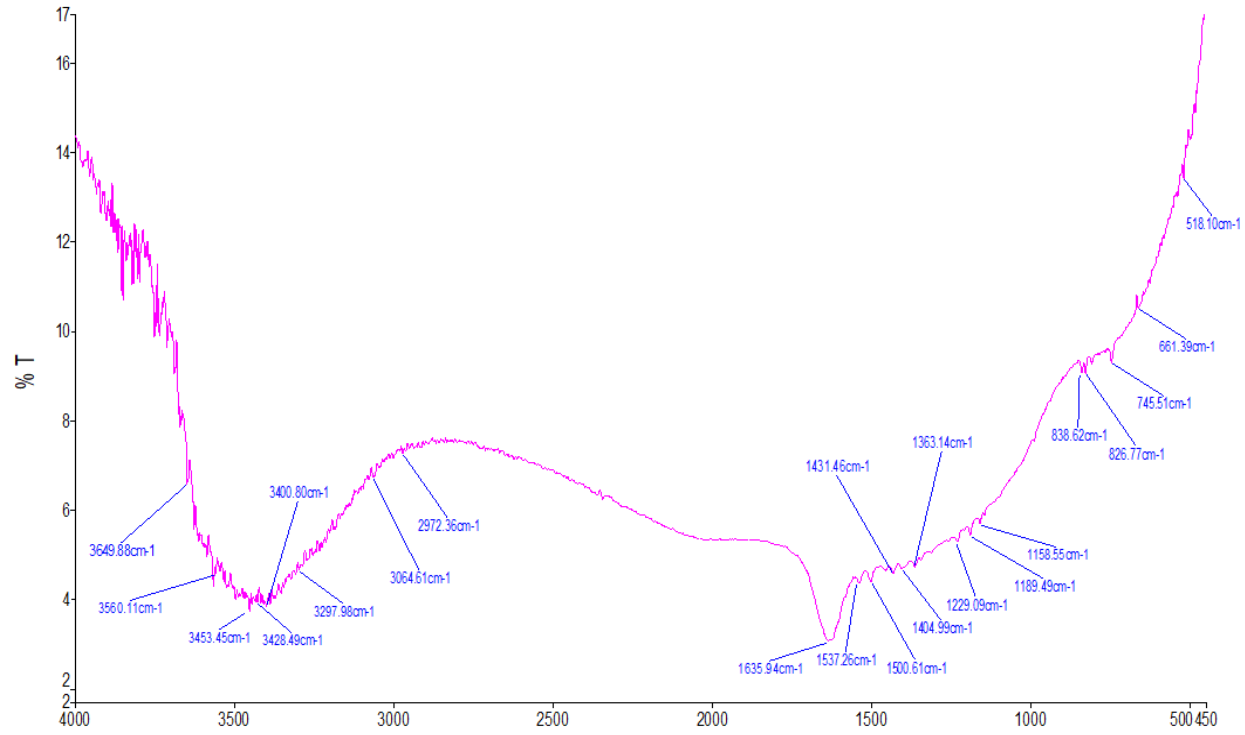

Appendix 6. illustrates the FT-IR spectrum of Zn(II) metal complexes.

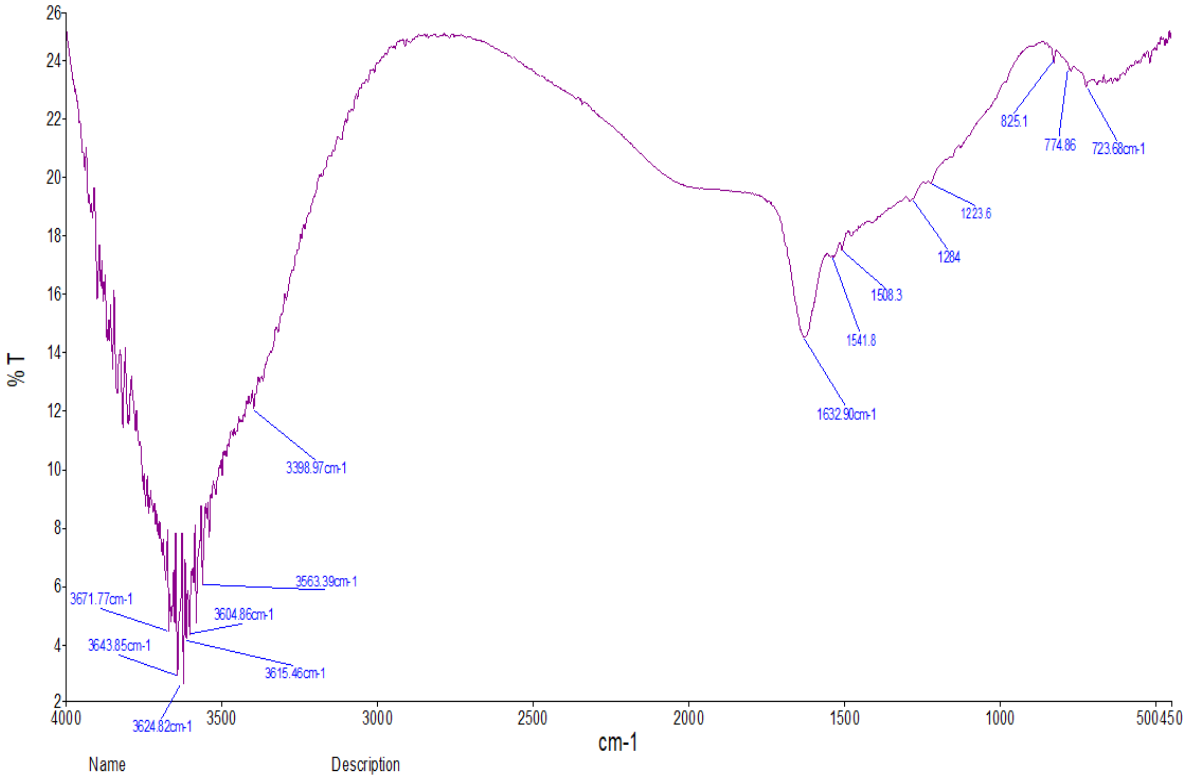

Appendix 7. illustrates the FT-IR- spectrum of the synthesized ligand.